Arch. Metall. Mater. **68** (2023), 2, 541-550

DOI: https://doi.org/10.24425/amm.2023.142433

U. MAGARAJAN[1*], S. SURESH KUMAR[2]

A COMPARATIVE STUDY ON BALLISTIC BEHAVIOUR OF MWCNT / GRAPHENE REINFORCED AL6061 SURFACE COMPOSITES FABRICATED VIA FRICTION STIR PROCESSING

In this work, a comparative study on the ballistic behaviour of friction stir processed AL6061 targets had been made. Base Metal AL6061 (BM) plates with 25 mm thickness were friction stir processed by adding Multi Walled Carbon Nano Tubes (MWCNT) and Graphene (G), producing AL6061-MWCNT and AL6061-G surface composites. Optical microscopy and microhardness test on BM, AL6061-MWCNT and AL6061-G samples were performed as per the standard procedure. It was noticed that uniform dispersion of ceramic particles and refined grains were obtained for the friction stir processed surface composites. From the microhardness test, it was perceived that friction stir processing had induced strengthening of surface composites, hence increasing the microhardness of AL6061-MWCNT and AL6061-G by ~60.3% and ~73.6% respectively. Also, ballistic experiments were conducted at 680±10 m/s by impacting Ø7.62×51 mm projectiles. AL6063 backing plates were placed to compare the ballistic behaviours AL6061-MWCNT and AL6061-G targets by depth of penetration. It was noted that the depth of penetration of AL6061-MWCNT and AL6061-G targets were 37.81% and 65.84% lesser than the BM target. Further, from the results of Post ballistic microscopy it was observed that the microstructure near and away from the penetration channel edge looks unchanged in BM target. However, the AL6061-MWCNT and AL6061-G targets showed considerable change in their morphology, by forming Adiabatic Shear Bands.

Keywords: Ballistic Behaviour; Friction Stir Processing; Graphene; Multi Walled Carbon Nano Tubes; Depth of Penetration

1. Introduction

Steel is universally recognised as the dominant material for the manufacturing of ballistic resistant military structures due to its typical features like high hardness, tensile property and energy absorbing capability [1-3]. However, because of its high density; light-weight materials like magnesium, titanium and aluminium alloys have reached massive interest among researchers to study on their ballistic behaviour [4-7]. Considering the low hardness of magnesium and high cost of titanium, aluminium alloys are accepted as a suitable alternate material for steel. Some of the reasons that make aluminium alloys a possibility for ballistic protection are its low density, moderate hardness and toughness. Despite its positive characteristics, it can be seen that a small Armour Projectile can completely penetrate the aluminium armour plates causing plugging, fragmentation, spalling and other modes of failures [8]. These failures occur since aluminium alloys do not have enhanced hardness in comparison to steel. To overcome this and make aluminium alloys a preferable armour material; Silicon Carbide, Boron Carbide, Graphene, Tungsten Carbide, Zirconium, Carbon Nano Tubes and other ceramic particles are generally used as reinforcements with aluminium matrix. These ceramic reinforced aluminium metal matrix composites had got enhanced hardness compared to commercially available aluminium alloy materials and hence, can emerge as an affordable material candidate for ballistic protective system. In order to develop ceramic reinforced metal matrix composites, many manufacturing processes are available such as stir casting, powder metallurgy, spraying, coating, CVD, Friction Stir Processing (FSP), sand witching, etc., [9-13]. Among the various manufacturing methods highlighted, FSP is a unique process to fabricate aluminium based surface composite [14].

Researchers had explored FSP on various aluminium alloys and tried to improve the mechanical properties like tensile strength and microhardness. Hossieni et al. [15] investigated the effect of incorporating CeO_2 and MWCNT particles into AL5083 matrix by FSP. Maximum microhardness was attained on hybrid composite containing CeO_2 and MWCNT in the ratio 25-75. The hybrid surface composite exhibited improved microhardness of 118% compared to the base metal. Khodabhakshi et al. [16] assessed the

[1] SRI VENKATESWARA COLLEGE OF ENGINEERING, CHENNAI, INDIA
[2] SRI SIVASUBRAMANIYA NADAR COLLEGE OF ENGINEERING, CHENNAI, INDIA
* Corresponding author: magarajan84@gmail.com

microhardness variation of AL5052 alloy by reinforcing MWCNT using FSP. Refined grains were obtained in AL5052-MWCNT surface composite, and as a result, the microhardness increased by two times. Also, Khodabhakshi et al. [17] investigated the influence of multi pass FSP on AL5052-Graphene surface composite. It was observed that reinforcement of graphene by FSP had produced grain refinement, and consequently, improved the microhardness from 55 HV to 84 HV. Zhenglin et al. [18] fabricated a novel AL-AL_2O_3-MWCNT composite by FSP, and observed that homogeneous dispersion of nano sized particles had resulted in significant improvement in the mechanical properties. The improvement in microhardness was related to grain refinement originated by the inclusion of ceramic particles. The microhardness modification of FSPed AL6061-SiC surface composites with impregnation of graphene and CNT was studied by Paul et al. [19]. It was concluded that the Orowan strengthening and hardness of graphene particles had significantly increased the microhardness of AL6061-SiC-Graphene surface composite by ~64.5%.

The noteworthy points from the literatures are; many researchers have explored the effect of Graphene and MWCNT on the mechanical characteristics of different series of aluminium alloys. However, the ballistic impact studies on FSPed surface composites have received less attention. Hence, in this present work, an attempt has been made to enhance the ballistic behaviour of AL6061 targets by reinforcing Multi-Walled CNT and Graphene via FSP technique. The microstructure, microhardness and ballistic behaviour of the surface composites are compared with the base metal.

2. Experimental methods

2.1. Materials and processing

Casted AL6061 plates (120×120×25 mm^3) are utilized as Base Metal (BM) in this study. The element composition and mechanical properties of the BM AL6061 are indexed in TABLE 1 and 2. AL6061 plates of dimensions 120×120 mm and thickness 25 mm are manufactured by stir casting process. Commercially available Multi Walled Carbon Nano Tubes (MWCNT, 99% pure, outer dia. 10-30 nm, inner dia. 5-10 nm, purchased from Ad-Nano Technologies, India) and Graphene (G, 99% pure, 5-10 layers, 5-10 nm thickness, purchased from Ad-Nano Technologies, India) are used as reinforcement materials. Fig. 1a and 1b show the SEM morphology with Raman spectra of MWCNT and Graphene particles.

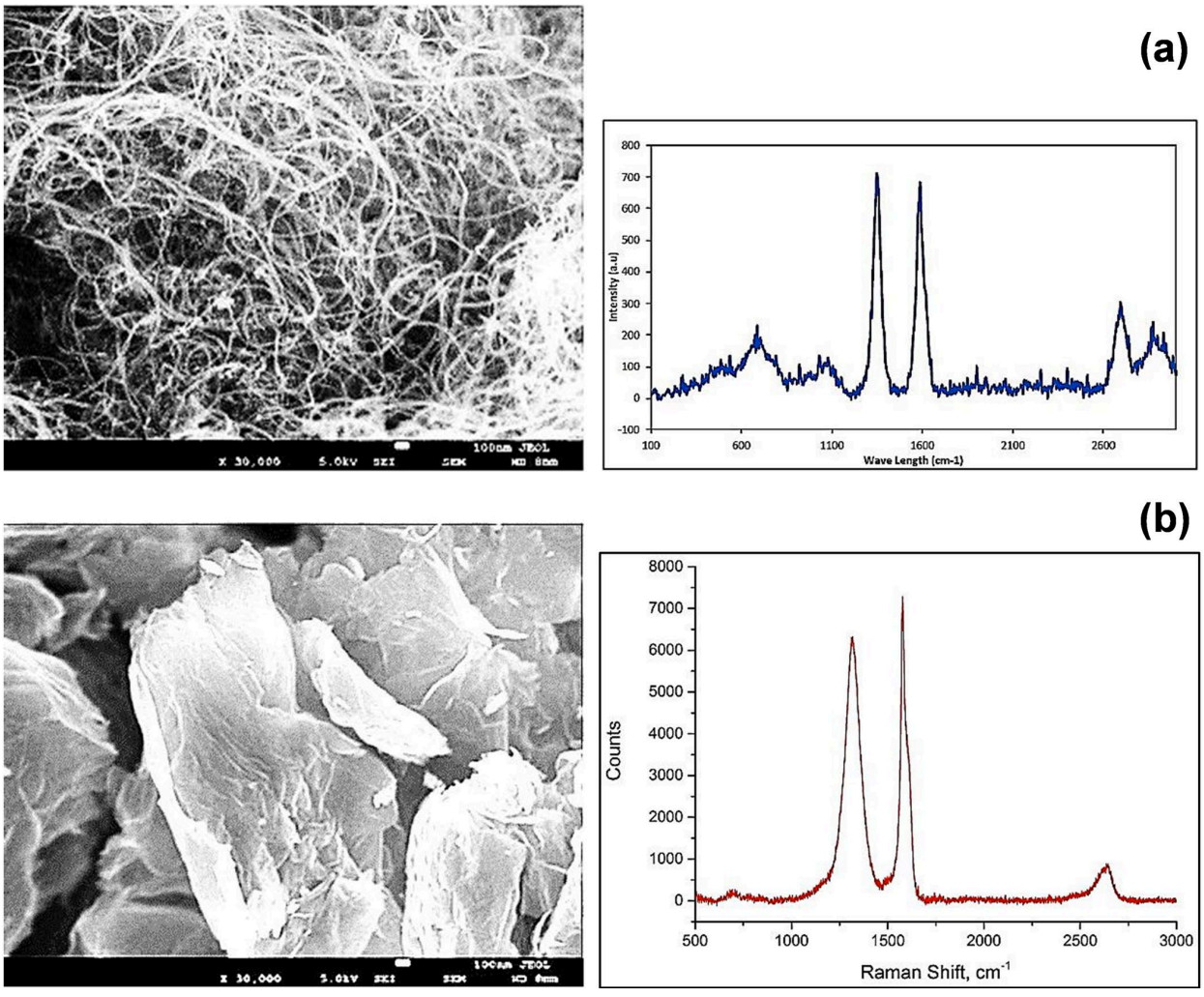

Fig. 1. SEM morphology with Raman Spectra of (a) MWCNT (b) Graphene

TABLE 1

Element composition of AL6061 (in wt. %)

AL6061 Elements	Si	Fe	Cu	Mn	Mg	Cr	Zn	Ti	Al
wt. %	0.539	0.262	0.259	0.049	0.870	0.127	0.057	0.011	97.76

TABLE 2

Mechanical properties of AL6061

Material	Tensile strength (MPa)	Modulus of Elasticity (GPa)	Mass density in Kg/m^3	Microhardness
AL6061	130	70	2700	68 HV

A long groove of dimension 2 mm width and 4.9 mm depth is formed on BM AL6061 plate using wire EDM. To enhance the microhardness and ballistic behaviour of BM AL6061, MWCNT and Graphene particles are filled separately in the groove. FSP is carried out on Friction Stir Welding machine using two tools; with and without pin. The FSP tools are machined of H13 steel with shoulder diameter 18mm and pin height 5 mm. To prevent the reinforcement particles from scattering, the tool without pin is first made to travel. Finally, the tool with squared pin profile is passed over the groove. Fig. 2 explains the details of the process involved in the fabrication of FSPed surface composite targets. Totally six FSPed target plates (3 nos. of AL6061-MWCNT and 3 nos. of AL6061-G) are processed at FSP parameters 1200 rpm and 50 mm/min. The fabricated surface composites are shown in Fig. 3. The smooth and flat crown appearance reveals the

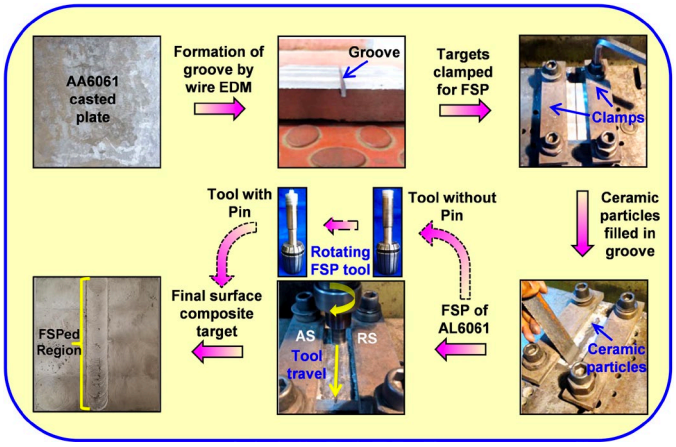

Fig. 2. Details of the process involved in the fabrication of FSPed surface composite targets

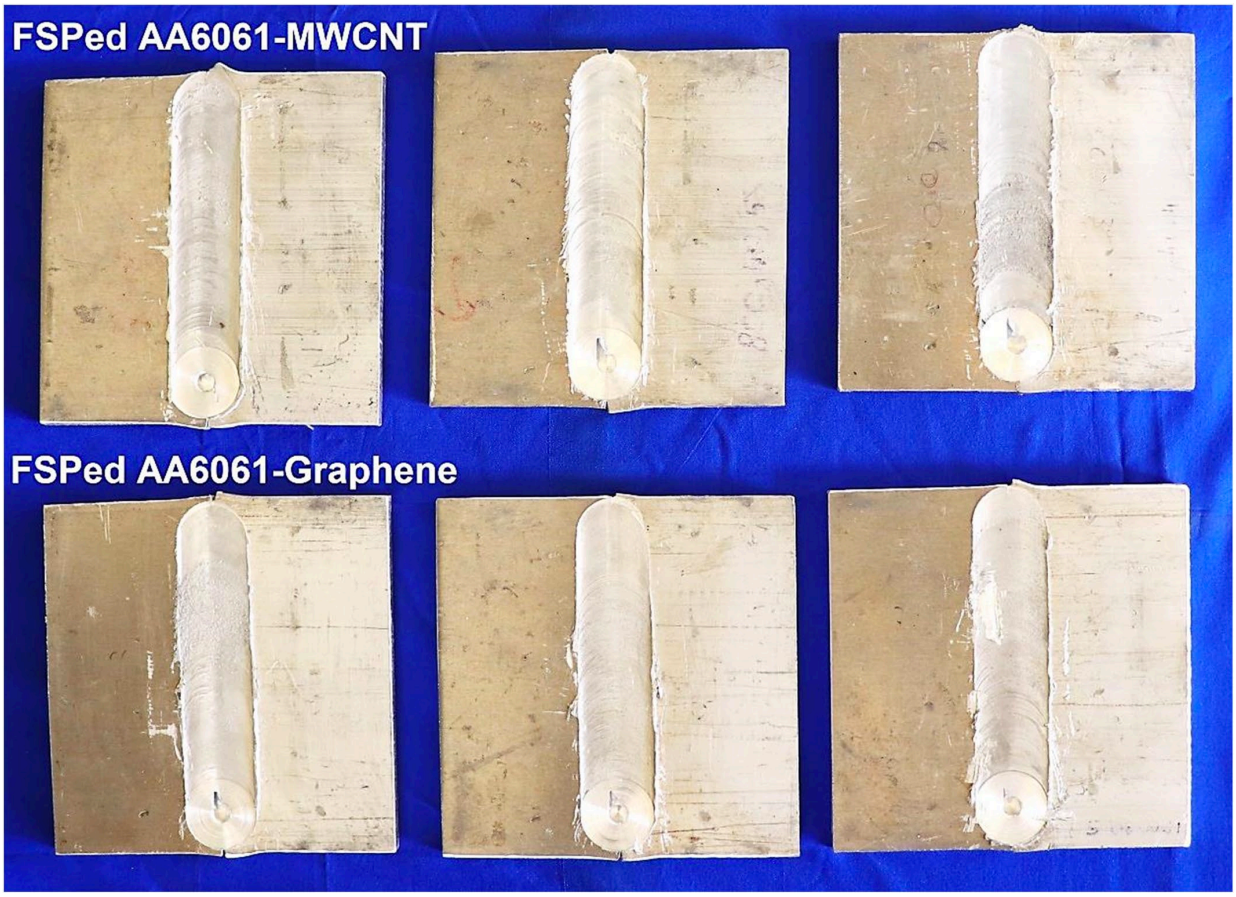

Fig. 3. Fabricated surface composite targets

TABLE 3

Details of the targets with corresponding acronym

S. No	Matrix + Reinforcement	Sample description	Acronym used in this study
1	AL6061 + No reinforcement	Base Metal AL6061	BM
2	AL6061 + Multi walled Carbon Nano Tubes	FSPed AL6061-MWCNT surface composite	AL6061-MWCNT
3	AL6061 + Graphene	FSPed AL6061-G surface composite	AL6061-G

formation of defect-free surface composite targets [20]. The details of the targets are presented in TABLE 3, and corresponding acronym will be used in rest of the paper.

2.2. Microstructural Characterization

The microstructural study of BM, AL6061-MWCNT and AL6061-G are carried out using Leica optical microscope-DM4000M LED model. The specimens are sliced, moulded and ground by a set of emery in increasing order of grit size 180 to 2000 followed by 3 and 0.5 µm diamond polishing. The polished samples are chemical etched by Keller's reagent for a holding time of 30 seconds. In the case of FSPed sample, the plate is hack-sawed across the transverse direction, and the centre portion of the FSPed region is processed for microstructural characterization.

2.3. Microhardness measurement

Microhardness measurements of BM, AL6061-MWCNT and AL6061-G targets are evaluated using Vickers microhardness (Matsuzawa-MMT X7) tester as per ASTM E384-17 standard [21]. The samples are acquired along the transverse direction to FSP. Microhardness readings are taken at equal interval of 1 mm in both advancing and retarding sides at a depth of 2 mm from the FSPed surface. An indentation load of 100 g and dwell time 15 second is maintained. All the tests are repeated 3 times, and the average value is computed.

2.4. Ballistic impact experiments

High velocity ballistic experiments are conducted on BM, AL6061-MWCNT and AL6061-G targets as per NIJ standard 0108.01 [22]. The schematic arrangement of the ballistic testing machine is shown in Fig. 4. The targets are clamped along with AL6063 backing plates of 25 mm thickness, and the ballistic behaviour is computed by Depth of Penetration (DoP) method. The targets are impacted against Ø7.62×51 mm Hard Steel Core (HSC) Projectiles at an initial velocity of 680±10 m/s. In between the target and the barrel, an infrared light emitting diode is placed to measure the projectile's velocity. The test is conducted for three samples and the average values are taken. The photographs of the projectile before and after impact are displayed in Fig. 5a and 5b.

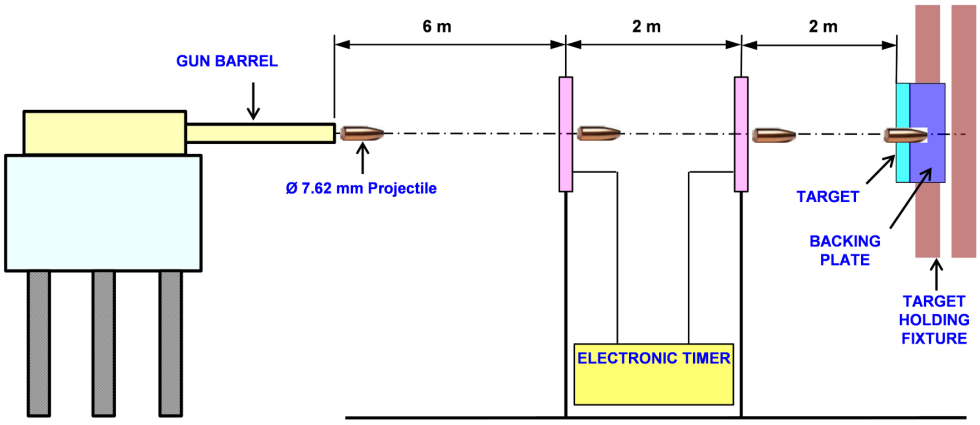

Fig. 4. Schematic diagram of ballistic testing machine

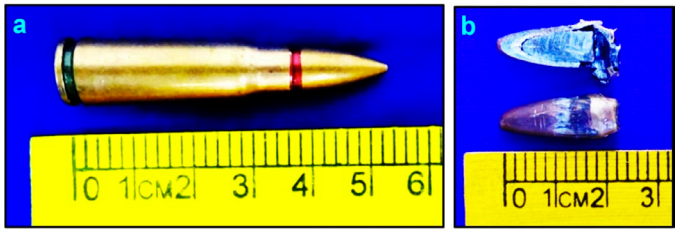

Fig. 5. Photographs of Ø7.62×51 mm HSC projectile (a) before impact (b) recovered projectile after penetration

3. Results and discussion

3.1. Microstructural analysis

The optical microscopy of BM is presented in Fig. 6. The microstructure is indicated by the presence of α-Al dendritic structure with quasi-globular morphology. The microstructural changes in AL6061-MWCNT and AL6061-G surface composites after FSP are shown in Fig. 7a and 8a. During the process of FSP,

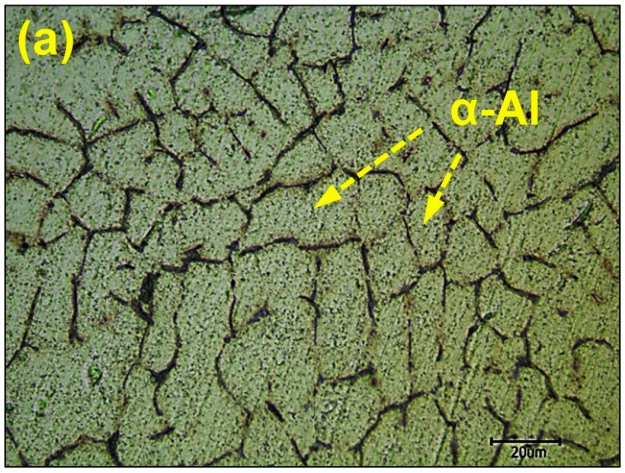

Fig. 6. Optical Microscopy of AL6061

the tool rotates and plunges into the groove of the material and travels along. This action stirs and blends AL6061 and reinforcement continuously, resulting in uniform distribution of CNT and G particles. At the time of FSP, the material is exposed to severe plastic deformation; consequently, MWCNT and G particles are fragmented and distributed into the α-aluminium matrix. Therefore, it can be inferred that the localized plastic deformation induced by FSP has improved the dispersion of ceramic particles within the FSPed region. The presence of MWCNT and Graphene particles are confirmed through EDS results as shown in Fig. 7b and 8b.

Moreover, by comparing the microstructural images (Fig. 6-8), it is explicit that, FSP has caused substantial grain refinement in both the surface composites. The grain size reduced from ~17.5 μm in the BM to ~5.9 and ~5.6 μm in the FSPed region of AL6061-CNT and AL6061-G samples. The grain refinement obtained in the FSP process is confirmed with the previously reported results on FSP of AL6061 alloys [23,24]. Therefore, severe plastic deformation along with dynamic recrystallization that occurs during FSP can be the reason for the grain refinement [25].

3.2. Microhardness of FSPed targets

Vickers microhardness test is carried out on the transverse side to FSPed direction. Fig. 9 represents the microhardness plot of AL6061-MWCNT and AL6061-G samples with ordinate displaying the microhardness value and abscissa displaying the distance from the centre of stir zone. Both Al6061-MWCNT and AL6061-G targets show significant enhancement in microhardness value compared to BM target.

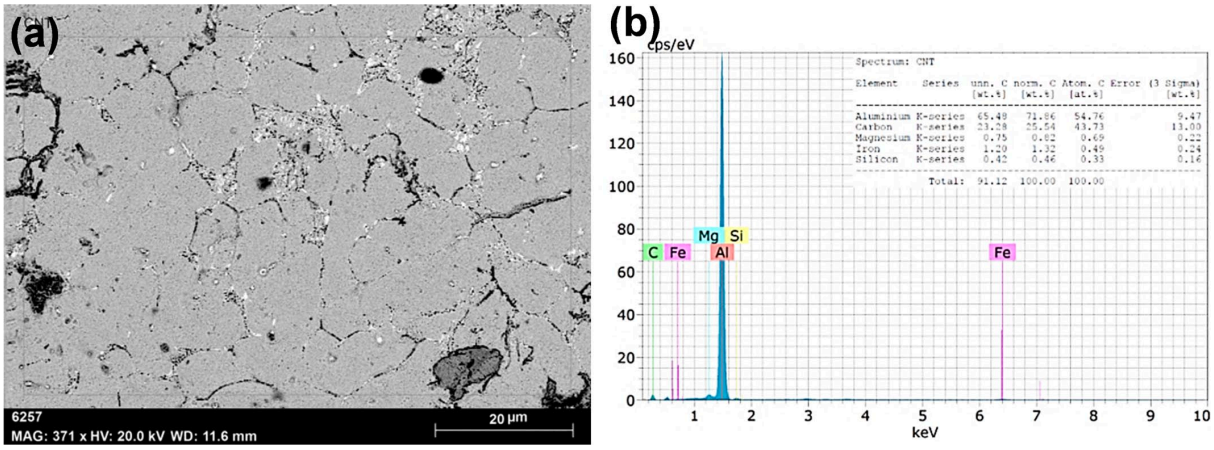

Fig. 7. AL6061-MWCNT (a) Microstructure (b) EDS spectra

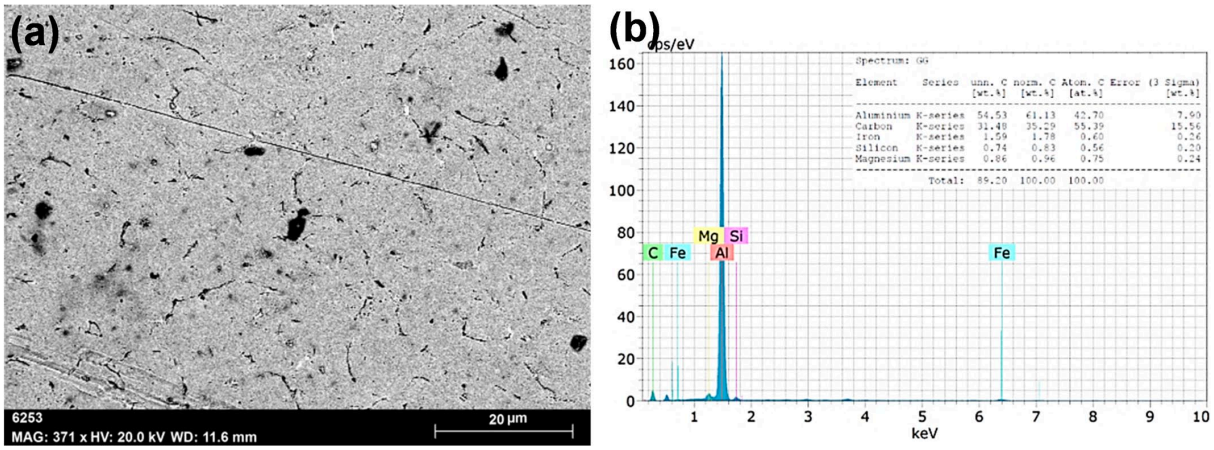

Fig. 8. AL6061-G (a) Microstructure (b) EDS spectra

AL6061-MWCNT target show an increase in microhardness of ~60.3% compared to the BM. An exceptional increase in microhardness of ~73.6% is obtained for AL6061-G target. From the microhardness graph, Fig. 9, it can be viewed that an asymmetrical distribution of microhardness contour is obtained. Higher microhardness values are attained on advancing side of the stir zone due to material flow from retreating side to advancing side during the FSP process.

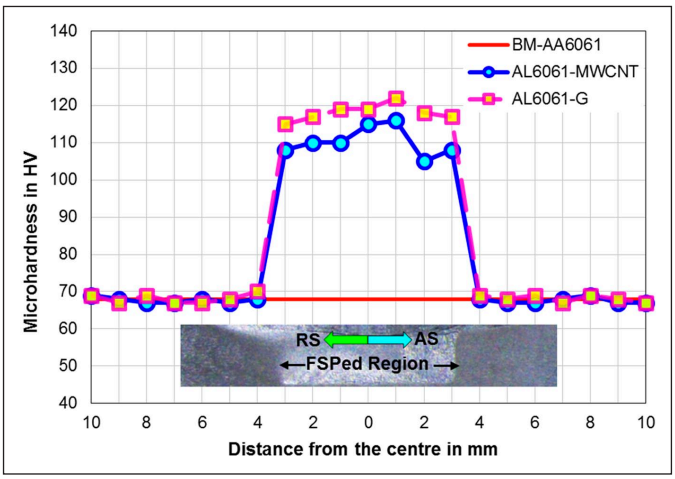

Fig. 9. Microhardness plot of AL6061-MWCNT and AL6061-G targets

In general, strengthening of metal matrix composite is primarily controlled by three strengthening mechanisms, i.e., Orowan strengthening, grain refinement and work hardening. For composites fabricated through FSP, all the three mechanisms participate considerably and enroute strengthening of the composite. Homogenous distribution of ceramic particles develops Orowan strengthening that contributes in improving the microhardness [26]. It is a widely known fact that the hardness of the ceramic particle is exceptionally high in comparison with the aluminium matrix; hence, blending of ceramic particles in BM improves the overall microhardness of the FSPed targets. Further, corresponding to Hall-Petch relation, the grain size dominates the mechanical characteristics of metals [25]. Due to grain refinement during FSP process, the grain size of AL6061-MWCNT and AL6061-G are smaller than BM as discussed in the preceding section. Therefore, these refined grains revive to enhance the microhardness. In addition, change in thermal contraction difference of AL6061 and ceramic particles produce work hardening effect [27].

As FSP is associated with intense plastic deformation, the rotating motion of the tool is capable to splash the ceramic particles, resulting in the above possible strengthening mechanisms. Thus, addition of ceramic particles, especially graphene, has significantly improved the microhardness of AL6061-G target.

3.3. Ballistic results

3.3.1. Measurement of ballistic behaviour

Fig. 10(a-c) show the closer view of the front face of BM, AA60601-MWCNT and AA6061-G targets after subjected to high velocity projectile impact. It can be spotted that the high velocity projectiles have completely penetrated and damaged the targets. After the projectile impact, all the backing plates are sectioned carefully along the penetration channel to measure the DoP. A video profile measuring instrument with an accuracy of ±0.005 mm is used to measure the DoP into the backing plates. The sectioned backing plates of AA6061-MWCNT and AA6061-G targets are shown in Fig. 11.

The average DoP in BM target is 16.45 mm, whereas, the average DoP in AL6061-MWCNT and AL6061-G targets are found to be 10.23 mm and 5.62 mm respectively. The DoP values of BM and FSPed targets are plotted in Fig. 12. It can be inferred that, compared to BM target, 65.84% lesser DoP is obtained for AL6061-G target. This indicates that the penetration resistance of the AL6061-G target is higher when compared with the BM target, hence yielding a better ballistic behaviour. The increase in ballistic behaviour can be directly correlated with the reinforcement of hard ceramic particles into AL6061 matrix during FSP.

From the published result [28], the frictional behaviour of target-projectile and the hardness of the target material are the

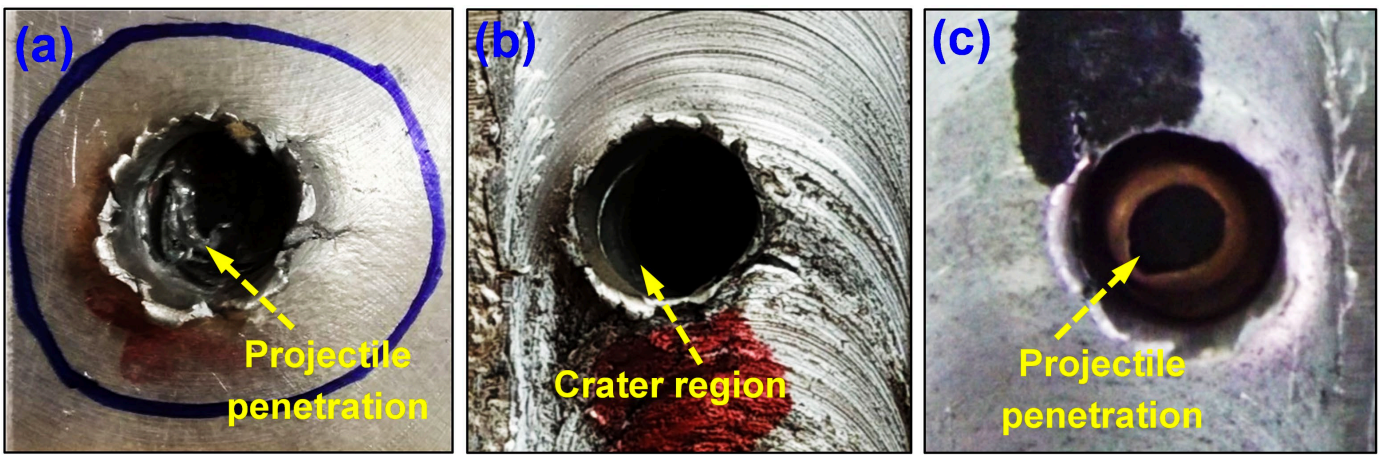

Fig. 10. Front face of targets after the ballistic test (a) BM (b) AL6061-MWCNT (c) AL6061-G

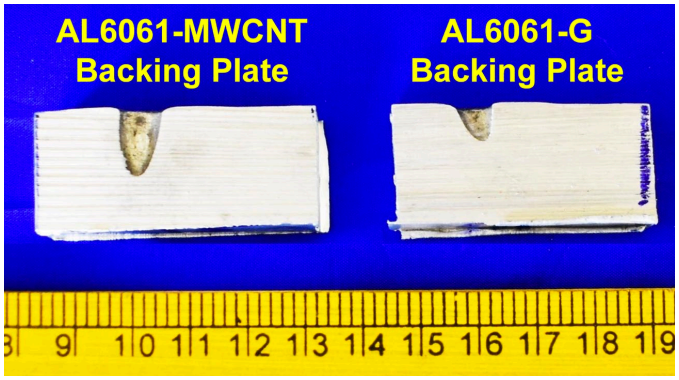

Fig. 11. Sectioned view of the backing plate of AL6061-MWCNT and AL6061-G targets

factors that vary the DoP during a ballistic impact. At the time of penetration, the abrasive motion between the ceramic particles and projectile's outer surface results in high friction. By this frictional characteristic, the kinetic energy of the projectile is dissipated over the target. This friction lowers the penetration depth, thus reducing the DoP of the FSPed targets. It can thus be concluded that stronger the friction between projectile and target, smaller will be the DoP.

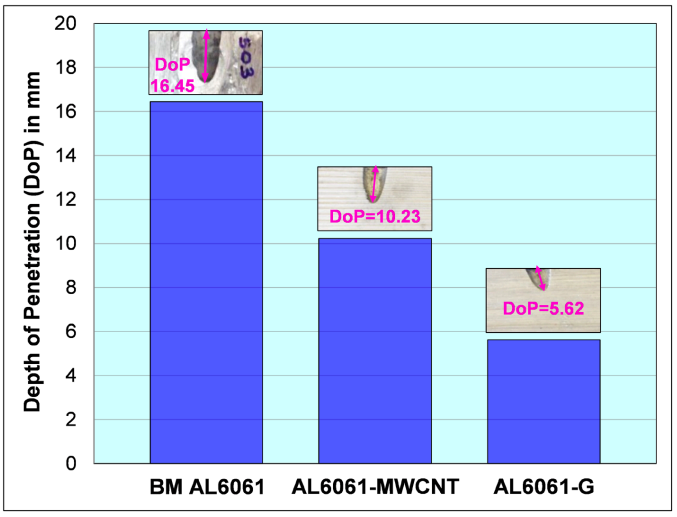

Fig. 12. DoP of BM, AL6061-MWCNT and AL6061-G targets

Moreover, uniform dispersion of hard ceramic particles has enhanced the microhardness of FSPed targets, thus increasing its resistance towards plastic flow during projectile impact. This too causes dissipation of kinetic energy of projectile and hence decreases the DoP. Compared to BM, 65.8% enhancement in ballistic behaviour is attained in AL6061-G target, while only 37.8% improvement in ballistic behaviour is noticed with AL6061-MWCNT target.

3.3.2. Formation of Adiabatic Shear Bands

Post ballistic optical microscopy is carried out to examine the microstructural changes around the crater region. The microstructures near the crater region and 10 mm away from the crater region are taken. The optical microscopy examination gives the identification of the ASBs along the edges of the penetration channel, which generally form in targets subjected to ballistic impacts. ASBs are usually recognised as a result from thermo-mechanical instability that leads to extreme deformation and high temperature in a narrow band. These bands are few tens of micrometres in width [29].

The optical microscopy in the vicinity of crater region (position 'a') and 10 mm away from the penetration channel (position 'b') are taken. Fig. 13 shows the microstructures of BM target near and away from the penetration channel edge. Both the microstructures look similar and doesn't feature any change. Fig. 14 and 15 represent the post ballistic microscopy of AL6061-MWCNT and AL6061-G targets. Here the microstructures near the penetration channel (position 'a' and 'c') feature considerable modification in their morphology after the ballistic impact. Especially in the entry region (position 'a') more change is noticed. It can be viewed that the grains are stretched along the edges of the penetration channel. This phenomenon is induced by high deformation around the crater region due to the projectile impact. Alike BM, it is noticed that the microstructures remain unaffected in the region far away from the projectile impact area (position 'b' and 'd'). These observations reveal that the interaction between the projectile and the target are limited to only few millimeters in close proximity to the penetration channel.

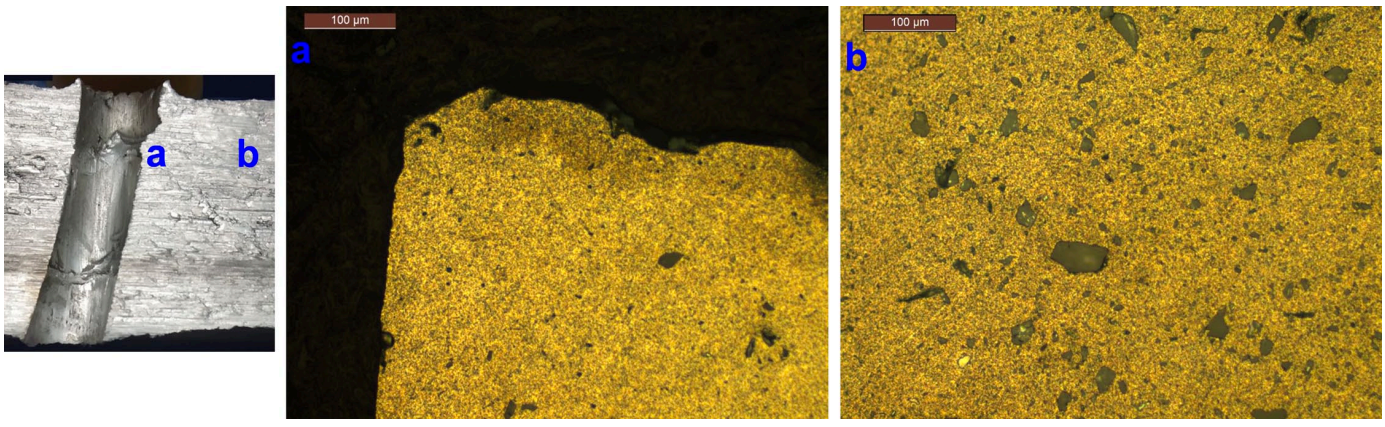

Fig. 13. ASB of BM (a) near the penetration channel (b) 10 mm away from penetration channel

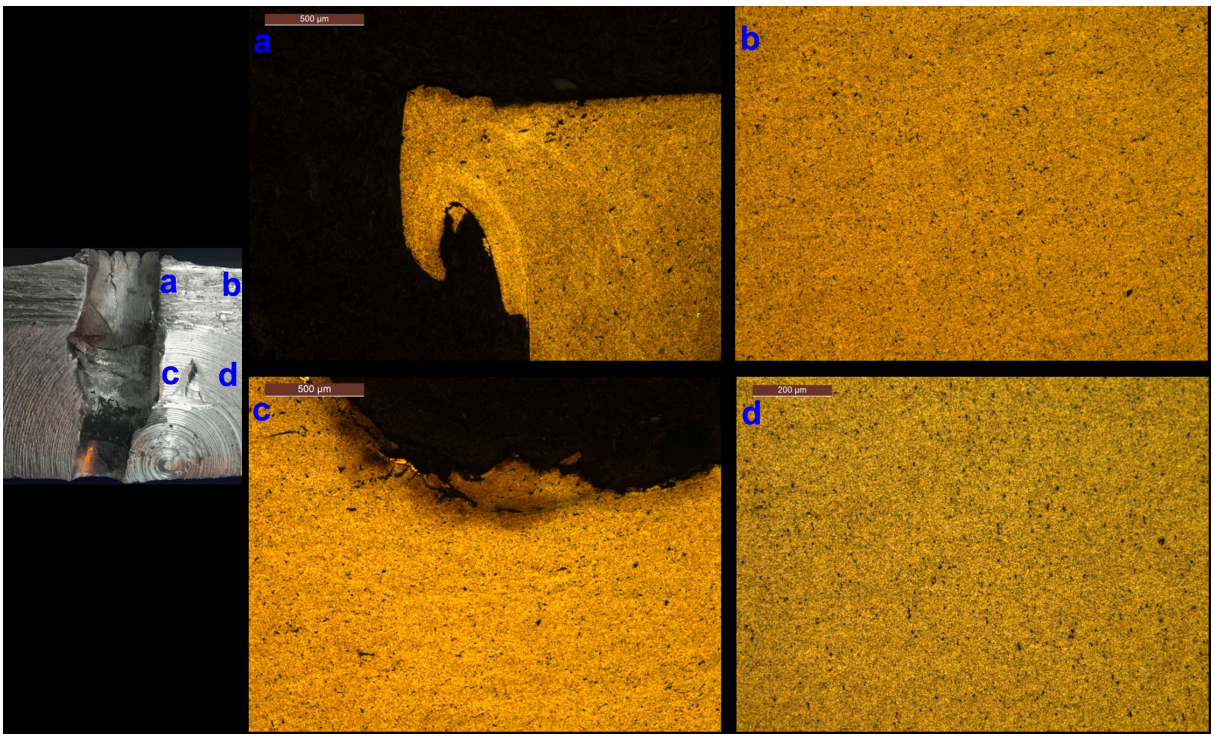

Fig. 14. ASB of AL6061-MWCNT (a) near the penetration channel (b) 10 mm away from penetration channel

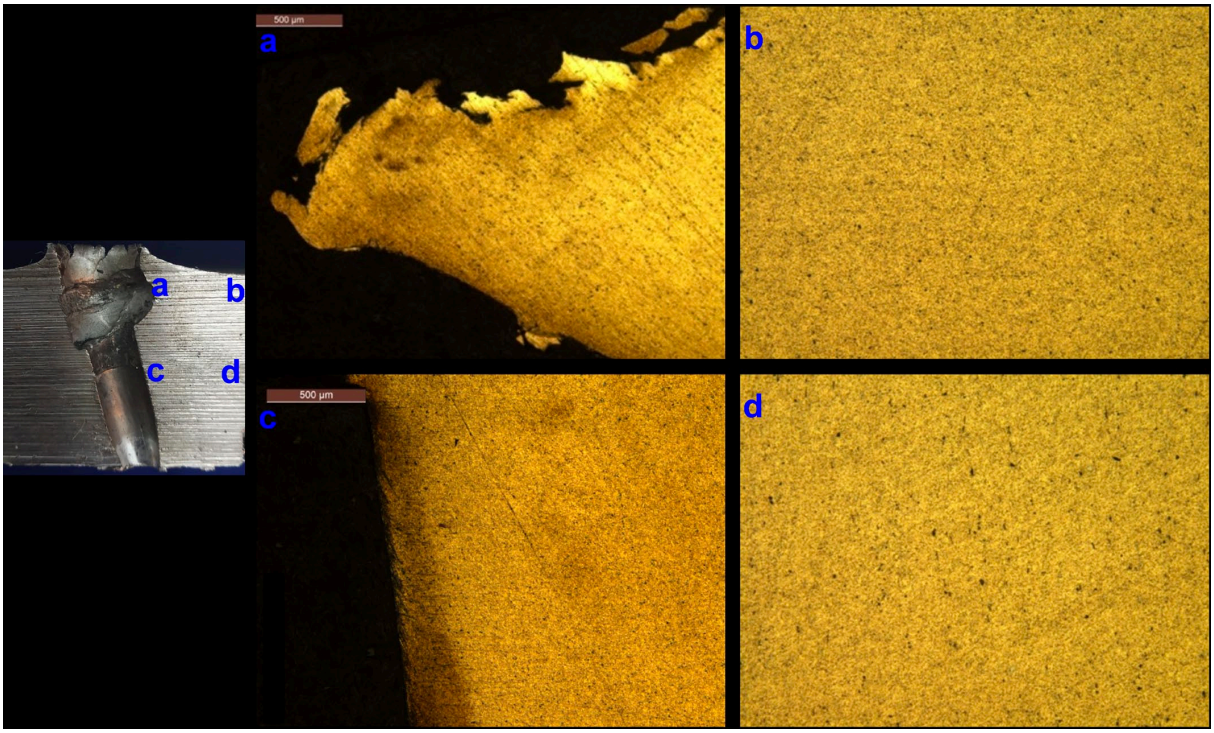

Fig. 15. ASB of AL6061-G (a) near the penetration channel (b) 10 mm away from penetration channel

ASBs are noticed in position 'a' of all the FSPed targets. The shear stress induced between the target and the projectile is the primary reason for the formation of ASBs. The ASBs in position 'a' are found to be more compared with position 'c'. Due to the high velocity of the projectile, the heat generated in some slip planes has insufficient time to dissipate the heat. Besides this, strain hardening takes place, causing a non-homogenous deformation in a set of bands [30]. These bands undergo instantaneous heating and then are cooled rapidly by the cool aluminium matrix around. As previously reported [31], the reason that make AA6061 good candidate for ballistic application is its good thermal conductivity rendering it less sensitive to ASB. Hence, the ASBs present in this work did not show any cracks formation from the shear bands.

4. Conclusion

A comparative study on the microhardness and ballistic behaviour of FSPed AL6061-MWCNT and AL6061-G targets were made by conducting ballistic experiments using Ø7.62×51 mm Armour Piercing Projectile at an ammunition range of 680±10 m/s. The following observations were inferred from the experimental work.

1. From the microstructural analysis, it was inferred that FSP had reduced the grain size of AL6061-CNT and AL6061-G surface composites significantly. Also, uniform dispersion of the ceramic particle was observed.
2. The microhardness of AL6061-MWCNT and AL6061-G samples were observed to be 109 HV and 118 HV respectively. Thus AL6061-G sample showed higher microhardness (~73.6% more) compared to BM.
3. The DoP in BM target was 16.45 mm, whereas, the DoP in AL6061-MWCNT and AL6061-G targets were 10.23 mm and 5.62 mm. It was inferred that, compared to BM target, 65.84% higher ballistic behavior was obtained for AL6061-G target.
4. The post ballistic microstructure near and away from the penetration channel edge looks unchanged in BM target. However, the AL6061-MWCNT and AL6061-G targets showed considerable change in their morphology, by forming ASBs. Especially in the entry region more changes were noticed.

REFERENCES

[1] F. Ade, Ballistic qualification of armor steel weldments, Welding J. **70** (9), 53-58 (1991).

[2] M.R. Edwards, A. Mathewson, The ballistic properties of tool steel as a potential improvised armour plate, Int. J. Impact Eng. **19** (4), 297-309 (1997).

[3] S. Mangenello, K.H. Abbott, Metallurgical factors affecting the ballistic behavior of steel targets, J. Mater. **7** (2), 231-239 (1972).

[4] U. Magarajan, S. Suresh Kumar, A Review Paper on Aluminium Targets Subjected to Ballistic Loading, J. Chem. Pharm. Sci. **7**, 39-44 (2017).

[5] S. Dharani Kumar, S. Suresh Kumar, A Review on Contact Ballistic Impact Studies on Monolithic Plate and Welded Joints, J. Chem. Pharm. Sci. **7**, 34-38 (2017).

[6] U. Magarajan, S. Suresh Kumar, Effect of ceramic particles reinforcement on the ballistic resistance of friction stir processed thick AA6061 surface composite targets. Proc. Inst. Mech. Eng., Part C: J. Mech. Eng. Sci. **235** (15), 2782-2794 (2020).

[7] R. Li, Q. Fan, R. Gao, L. Huo, F. Wang, Y. Wang, Effects of dynamic mechanical properties on the ballistic performance of a new near-β titanium alloy Ti684, Mater. Des. **62**, 233-240 (2014).

[8] M.E. Backman, W. Goldsmith, The mechanics of penetration of projectiles into targets, Int. J. Eng. Sci. **16** (1), 1-99 (1978).

[9] P. Shao, G. Chen, W. Yang, Q. Zhang, B. Ju, Z. Wang, X. Tan, Y. Pei, S. Zhong, M. Hussain, G. Wu, Effect of hot extrusion temperature on graphene nanoplatelets reinforced Al6061 composite fabricated by pressure infiltration method, Carbon **162**, 455-464 (2020).

[10] P.A. Vityaz, A.P. Ilyushchanka, V.V. Savich, Powder Metallurgy in Belarus and Global Developmental Trends, Russ. J. Non-ferrous Met. **60**, 775-781 (2019).

[11] M. Tabandeh-Khorshid, P.A. Kumap, E. Omrani, C. Kim, P. Rohatgi, Synthesis, characterization, and properties of graphene reinforced metal-matrix nanocomposites, Composites, Part B, **183**, 107664 (2020).

[12] P.A. Kumar, H.C. Madhu, A. Pariyar, C.S. Perugu, S.V. Kailas, U. Garg, P. Rohatgi, Friction stir processing of squeeze cast A356 with surface compacted graphene nanoplatelets (GNPs) for the synthesis of metal matrix composites, Mater. Sci. Eng. A **769**, 138517 (2020).

[13] E. Özşahin, S. Tolun, Influence of surface coating on ballistic performance of aluminum plates subjected to high velocity impact loads, Mater. Des. **31** (3), 127683 (2010).

[14] R. Bauri, D. Yadav, Metal matrix composites by friction stir processing. Butterworth-Heinemann, (2017).

[15] S.A. Hosseini, K. Ranjbar, R. Dehmolaei, A.R. Amirani, Fabrication of Al5083 surface composites reinforced by CNTs and cerium oxide nano particles via friction stir processing, J. Alloys Compd. **622**, 725-733 (2015).

[16] F. Khodabakhshi, A.P. Gerlich, P. Švec, Reactive friction-stir processing of an Al-Mg alloy with introducing multi-walled carbon nano-tubes (MW-CNTs): microstructural characteristics and mechanical properties, Mater. Charact. **131**, 359-373 (2017).

[17] F. Khodabakhshi, S.M. Arab, P. Švec, A.P. Gerlich, Fabrication of a new Al-Mg/graphene nanocomposite by multi-pass friction-stir processing: dispersion, microstructure, stability, and strengthening, Mater. Charact. **132**, 92-107 (2017).

[18] Z. Du, M.J. Tan, J.F. Guo, Fabrication of a new Al-Al_2O_3-CNTs composite using friction stir processing (FSP), Mater. Sci. Eng. A **667**, 125-131 (2016).

[19] A. Sharma, D. Narsimhachary, V.M. Sharma, B. Sahoo, J. Paul, Surface modification of Al6061-SiC composite through impregnation of graphene & carbon nanotubes via FSP: A tribological study, Surf. Coat. Technol. **368**, 175-191 (2019).

[20] U. Magarajan, S. Suresh Kumar, Experimental ballistic performance of friction stir processed aluminum (AA6061-B_4C) surface composite, Mech. Based Des. Struct. Mach. (2021).
DOI: https://doi.org/10.1080/15397734.2021.1913419

[21] ASTM E384-17, Standard test methods for Microindentation hardness of materials, ASTM International.

[22] K. James Stewart, Director. National Institute of Justice Ballistic Resistant Protective Materials (1985).

[23] I. Dinaharan, R. Nelson, S.J. Vijay, Microstructure and wear characterization of aluminum matrix composites reinforced with industrial waste fly ash particulates synthesized by friction stir processing, Mater. Charact. **118**, 149-158 (2016).

[24] A. Dorbane, B. Mansoor, G. Ayoub, Mechanical, microstructural and fracture properties of dissimilar welds produced by friction stir welding of AZ31B and Al6061, Mater. Sci. Eng. A **651**, 720-733 (2016).

[25] Z. Du, M.J. Tan, J.F. Guo, G. Bi, J. Wei, Fabrication of a new Al-Al_2O_3-CNTs composite using friction stir processing (FSP), Mater. Sci. Eng. A, **667**, 125-131 (2016).

[26] D.J. Lloyd, Particle reinforced aluminium and magnesium matrix composites, Int. Mater. Rev. **62** (1), 1-23 (2013).

[27] R. Casati, M. Vedani, Metal matrix composites reinforced by nano-particles – A review, Metals **4**, 65-83 (2014).

[28] M.B. Karamis, A. Tasdemirci, Nair FE, Failure and tribological behaviour of the AA5083 and AA6063 composites reinforced by SiC particles under ballistic impact, Composites, Part A, **34** (3), 217-226 (2003).

[29] D.H. Li, Y. Yang, T. Xu, H.G. Zheng, Q.S Zhu, Q.M. Zhang, Observation of the microstructure in the adiabatic shear band of 7075 aluminum alloy, Mater. Sci. Eng. A **527**, 3529-3535 (2010).

[30] A. Manes, M. Pagani, M. Saponara, D. Mombelli, C.A. Mapelli, M. Giglio, Metallographic characterisation of Al6061-T6 aluminium plates subjected to ballistic impact, Mater. Sci. Eng. A **608**, 207-220 (2014).

[31] T. Børvik, A.H. Clausen, M. Eriksson, T. Berstad, O.S. Hopperstad, M. Langseth, Experimental and numerical study on the perforation of AA6005-T6 panels, Int. J. Impact Eng. **32**, 35-64 (2005).